# Dual-band frequency selective surface with quasi-elliptic bandpass response*

Zhou Hang(周 航)[a], Qu Shao-Bo(屈绍波)[a]†, Peng Wei-Dong(彭卫东)[b], Wang Jia-Fu(王甲富)[a], Ma Hua(马 华)[a], Zhang Jie-Qiu(张介秋)[a], Bai Peng(柏 鹏)[b], and Xu Zhuo(徐 卓)[c]

[a] *College of Science, Air Force Engineering University, Xi'an* 710051, *China*
[b] *Synthetic Electronic Information System Research Department, Air Force Engineering University, Xi'an* 710051, *China*
[c] *Electronic Materials Research Laboratory, Key Laboratory of the Ministry of Education, Xi'an Jiaotong University, Xi'an* 710049, *China*

(Received 4 September 2010; revised manuscript received 2 September 2011)

Based on the substrate integrated waveguide technology, we present a dual-band frequency selective surface (FSS) with a quasi-elliptic bandpass response. The characteristics of the quasi-elliptic bandpass response are realized by shunting two substrate integrated waveguide cavities of different sizes, with the same slots on both sides of the metal surfaces. Four cavities of different sizes and two slots of different sizes are used to design the novel FSS. Every bandpass response with sharp sidebands is induced by two transmission nulls that are generated by the coupling between the slot aperture resonance and the cavity resonance. The simulation results show that such dual-band FSS has the advantages of high selectivity and stable performance at different oblique incident angles. Moreover, it is easy to fabricate.

**Keywords:** dual-band frequency selective surface, substrate integrated waveguide, quasi-elliptic bandpass

**PACS:** 03.50.De, 41.20.–q **DOI:** 10.1088/1674-1056/21/3/030301

## 1. Introduction

Frequency selective surfaces (FSSs) are periodic surfaces, which are composed of identical elements arranged in one- or two-dimensional finite arrays in practice.[1] There is continuing interest in the FSSs for more than four decades because of their comprehensive applications, such as polarizer, fliter, subreflector, and band-pass hybrid radome.[1−5] In some applications, multi-band FSSs have been used to design dual-reflector antennas. Such multi-band FSSs have made it possible to share the main reflector among different frequency bands.[6−8] With the development of modern communication technology, multi-band FSSs have gradually become a hot topic in the area of communication and have been investigated extensively. The ring and square loop elements have been used to construct the multi-band FSSs.[8,9] Two FSSs cascaded on complementary surface layers were discussed in Ref. [10]. Fractal elements were proposed to design multi-band FSSs.[11−13] Substrate integrated waveguide (SIW) technology was proposed by Luo *et al.*[14] to design FSSs, in which the SIW cavity is formed by arranging metal via an array around every periodic slot. The FSSs based on SIW technology can introduce a special cavity resonance with the remaining existing conventional slot resonance. Thus, a highly selective FSS with a sharp transition band can be easily realized by adjusting the coupling level between these two different resonances. Based on this method, FSSs with a quasi-elliptic bandpass response and much higher selectivity were designed.[15,16] Driven by the demand of the multi-band FSSs with higher selectivity, we use a structure proposed in Ref. [14] to design a novel FSS. The FSS exhibits dual-band quasi-elliptic bandpass response in each passband and stable per-

*Project supported by the National Natural Science Foundation of China (Grant Nos. 60871027, 60901029, and 61071058), the National Basic Research Program of China (Grant No. 2009CB623306), the Research Fund of Shaanxi Key Laboratory of Electronic Information System Integration, China (Grant No. 201114Y11), and the Postdoctoral Science Foundation of China (Grant No. 20100481327).

†Corresponding author. E-mail: Qushaobo@mail.xjtu.edu.cn

© 2012 Chinese Physical Society and IOP Publishing Ltd

formance for different incident angles.

## 2. Design

An FSS with a single quasi-elliptic passband can be realized by two cascaded cavities of different sizes.[15] However, it is hard to fabricate two-layered SIW cavity FSSs (SIWC-FSSs) for printed circuit board technology. For this reason, a single-passband FSS with a quasi-elliptic response was designed by shunting two SIW cavities of different sizes, with the same slots on both sides of the metal surfaces.[17] Accordingly, we may get a dual-band FSS with a quasi-elliptic bandpass response by shunting four SIW cavities of different sizes and two slots of different sizes. By adjusting the coupling level between the cavity and slot resonances, the characteristics of quasi-elliptic bandpass response will be realized. Based on this idea, the designed dual-band SIWC-FSS structure is shown in Fig. 1 and its 3-dimensional (3D) view is given in Fig. 2. The grid slots in Figs. 1(a) and 1(b) have the same dimensions, and only the cavity size is different. The case in Figs. 1(c) and 1(d) is the same as that in Figs. 1(a) and 1(b). Therefore, there are four cavities of different sizes and two slots of different sizes in Fig. 1.

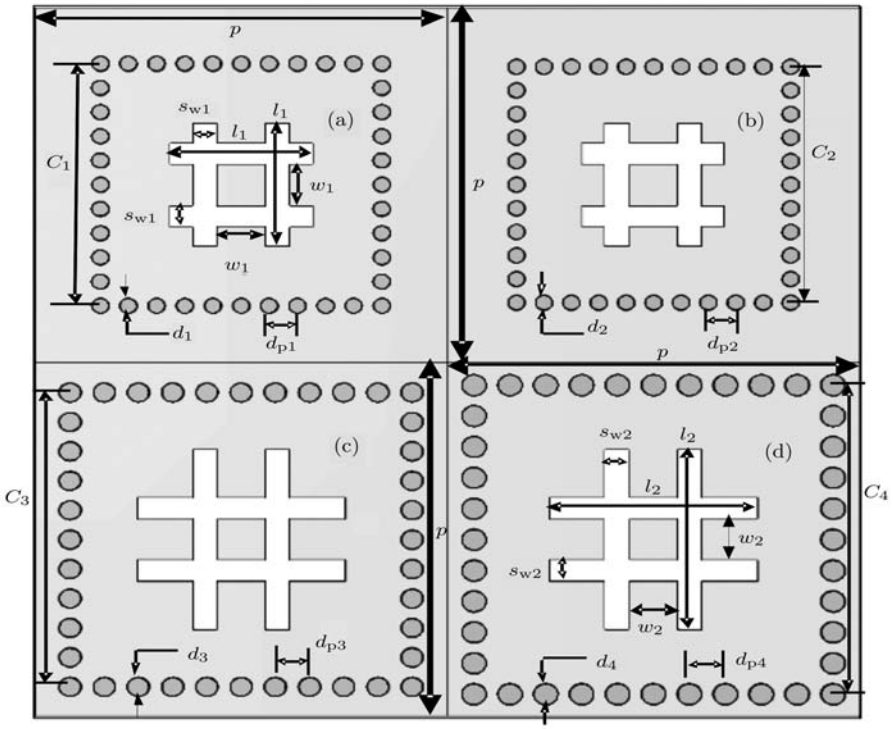



**Fig. 1.** An SIWC-FSS with a dual band quasi-elliptic bandpass realized by four different sized cavities shunting in neighbouring cells. Here, $p$ is the periodicity of the structure, $l_1$ is the length of the smaller grid slot, $s_{w1}$ is the width of the smaller grid slot, $l_2$ is the length of the larger grid slot, $s_{w2}$ is the width of the larger grid slot, $d_1$, $d_2$, $d_3$ and $d_4$ are the diameters of the metallic stubs, $d_{p1}$,$d_{p2}$, $d_{p3}$ and $d_{p4}$ are the spacing between neighbouring stubs. Specific values of the parameters are listed in Table 1. Panels (a),(b),(c),(d) represent four different unit structures.

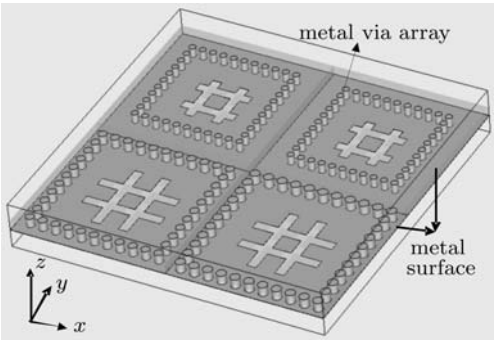



**Fig. 2.** 3D view of the SIWC-FSS.

The geometrical dimensions of the structure are given in Table 1. The FSS arrays have a substrate with a relative permittivity ($\varepsilon_r$) of 2.65, a loss tangent of 0.001, and a thickness $h$ of 1 mm.

We used the CST microwave studio based on the full wave simulation method, finite integration method (FIM), to calculate its reflection and transmission characteristics. We assume that the FSS is an infinite periodic structure. The FSS is excited by an incident plane wave with different polarizations at different incident angles. We adopt the periodic

**Table 1.** Geometrical parameters of FSS.

| Parameter | Value | Parameter | Value |
|---|---|---|---|
| $\varepsilon_{\rm r}$ | 2.65 | $d_3$/mm | 0.9 |
| $p$/mm | 17 | $d_4$/mm | 1 |
| $l_1$/mm | 5.87 | $d_{\rm p1}$/mm | 1.16 |
| $l_2$/mm | 8.6 | $d_{\rm p2}$/mm | 1.13 |
| $_{\rm w1}$/mm | 2 | $d_{\rm p3}$/mm | 1.41 |
| $_{\rm w2}$/mm | 2 | $d_{\rm p4}$/mm | 1.48 |
| $s_{\rm w1}$/mm | 1 | $C_1$/mm | 11.6 |
| $s_{\rm w2}$/mm | 1 | $C_2$/mm | 11.3 |
| $d_1$/mm | 0.7 | $C_3$/mm | 14.1 |
| $d_2$/mm | 0.7 | $C_4$/mm | 14.8 |

boundary conditions on the four sides of the unit cell. Figure 3 shows the simulated transmission and reflection characteristics at normal incidence. From Fig. 3(b), we can find two evident quasi-elliptic bandpass responses. Bandwidths of the lower and upper passbands are 410 MHz (11.31–11.72 GHz) and 430 MHz (15.78–16.21 GHz), respectively. The transition bandwidths of both lower and upper sharp sidebands (from –3 to –20 dB) of the lower quasi-elliptic passband are 20 MHz (11.29–11.31 GHz and 11.74–11.76 GHz). In addition, the transition bandwidths of the lower and upper sharp sidebands (from –3 to –20 dB) of the upper quasi-elliptic passband are also 20 MHz (15.75–15.77 GHz and 16.22–16.24 GHz). The pole of a conventional

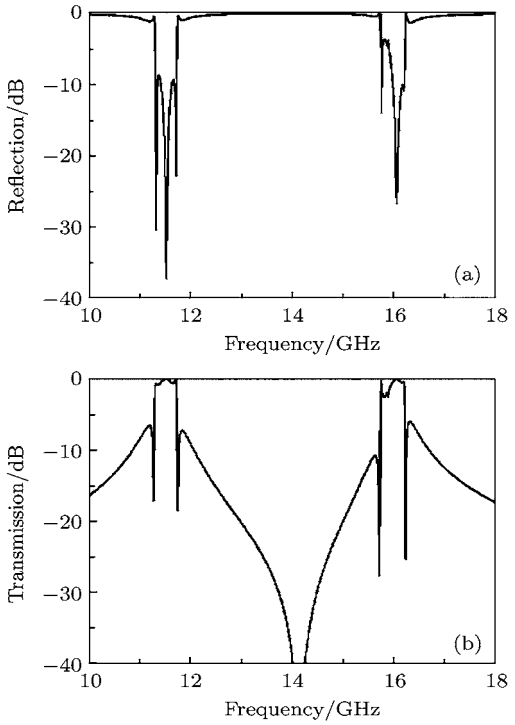



**Fig. 3.** Simulated reflection (a) and transmission (b) characteristics at normal incidence.

FSS at 14.15 GHz is generated by the coupling between the two # shape size slots. The transmission peak values of the SIWC-FSS at 11.32, 11.72, 15.75, and 16.2 GHz are generated by the coupling between the periodic slot resonance and the cavity resonance, which leads to a rapid roll-off sideband to emerge and a high selectivity of frequency.

## 3. Analysis

To reveal the mechanism of the SIWC-FSS, we present in Fig. 4 the diagrams of the electric field distribution at different frequencies in the two passbands. The diagrams (a), (b), (c), (d), (e), and (f) correspond to the resonances at 11.72, 11.5, 11.31, 15.78, 16.0, and 16.21 GHz, respectively.

The lower quasi-elliptic bandpass response can be revealed by Fig. 5. It is the response of the larger units (3) and (4) in Fig. 4(a). The upper (11.72 GHz) and lower (11.31 GHz) sharp sidebands in Fig. 5 are generated by the cavity resonances in units (3) and (4), respectively. The two cavity resonances can be seen in Figs. 4 (a) and 4 (c). It can be found in Fig. 4(a) that only distorted $TE_{120}$ cavity resonance occurs in unit (3) at 11.72 GHz. Similar phenomena can be seen in Fig. 4(c), while another cavity resonance occurs in unit (4) at 11.31 GHz. The bandpass frequency response between the two cavity resonances can be explained by Fig. 4(b). However, the electromagnetic energy is transmitted by the aperture resonance in both units (3) and (4). The couplings between these cavity and aperture resonances lead to the lower and upper sharp sidebands and a quasi-elliptic passband. Thus, by shunting units (3) and (4), we obtain a quasi-elliptic bandpass response.

The same situation can be applied to the upper quasi-elliptic bandpass response that is shown in Fig. 6. Under similar conditions, another quasi-elliptic passband is generated by units (1) and (2). It can be observed from Figs. 4(d) and 4(f) that at 15.78 and 16.21 GHz, two distorted $TE_{120}$ cavity resonances occur in units (1) and (2), respectively. Aperture resonances occur in both unit (1) and (2) at 16.0 GHz. The transmission null of the SIWC-FSS at 14.14 GHz is generated by the coupling between two aperture resonances of different sizes, which can be shown in Figs. 4(b) and 4(e). Consequently, when the four units (1), (2), (3), and (4) are shunted together, a dual-band FSS with quasi-elliptic bandpass response can be obtained.

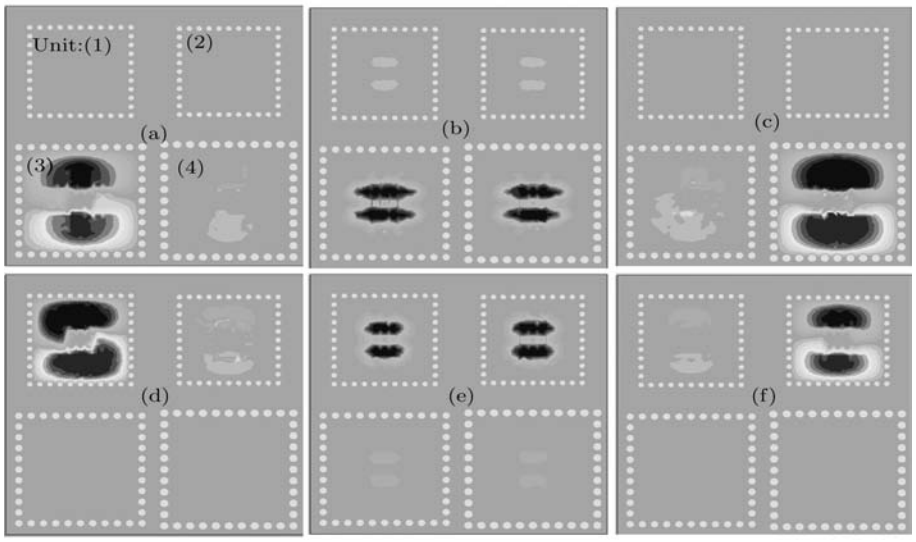



**Fig. 4.** Electric field distribution diagrams at different frequencies: (a) 11.31 GHz, (b)11.5 GHz, (c)11.72 GHz, (d)15.78 GHz, (e)16.0 GHz, and (f)16.21 GHz. Units (1), (2), (3), (4) are structures corresponding to Figs. 1(a), 1(b), 1(c), and 1(d), respectively.

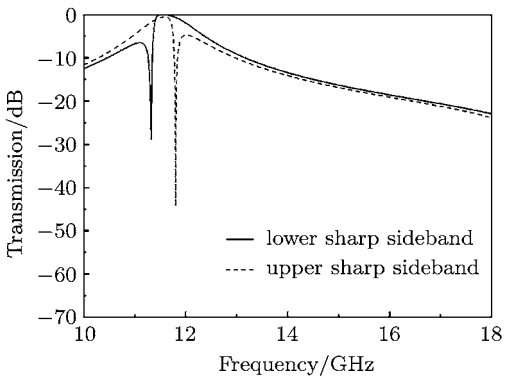



**Fig. 5.** Lower passband frequency response of SIWC-FSS with two cascaded cavities of different sizes.

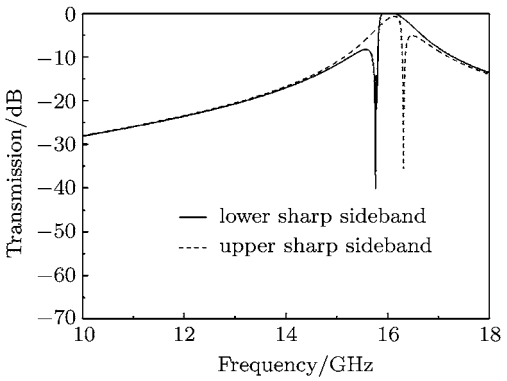



**Fig. 6.** Upper passband frequency response of SIWC-FSS with two cascaded cavities of different sizes.

Figure 7 gives the frequency responses at different incident angles. The incident plane wave vector $\boldsymbol{k}$ is fixed in the $x$–$z$ plane and the electric field vector $\boldsymbol{E}$ is fixed in the $y$ direction. From Fig. 7, we can find that the resonance frequency of FSS is rather stable under oblique incident angles from 0° to 30°. The bandwidth ratio of different incident angles is very close to 1.0. Therefore, the dual-band FSS with quasi-elliptic bandpass response owes its advantages to high selectivity and stable performance.

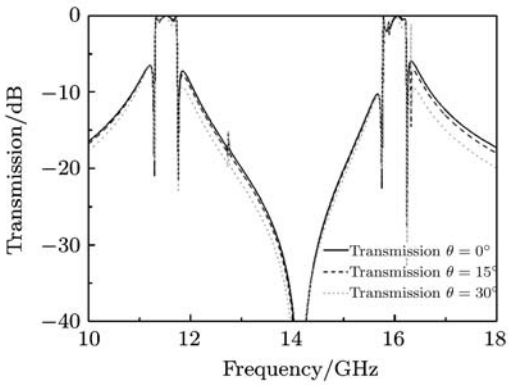



**Fig. 7.** Simulated transmission characteristics at various incident angles $\theta$.

## 4. Conclusions

In this paper, we propose a dual-band FSS with a quasi-elliptic bandpass response in every passband. The characteristics of a quasi-elliptic bandpass response are realized by shunting two SIW cavities of different sizes, with the same slots on both sides of the metal surfaces. The proposed FSS has the advantages of high selectivity and stable performance at different incident angles. By virtue of these advantages, the proposed FSS can provide practical applications

to modern communication technology and electronic countermeasures, etc.

# References


[1] Munk B A 2000 *Frequency Selective Surfaces: Theory and Design* (New York: Wiley)

[2] Wu T K 1995 *Frequency Selective Surface and Grid Array* (New York: Wiley)

[3] Li X Q, Gao J S, Zhao J L and Sun L C 2008 *Acta Phys. Sin.* **57** 3803 (in Chinese)

[4] Jia H Y, Gao J S, Feng X G and Sun L C 2009 *Acta Phys. Sin.* **58** 505 ( in Chinese)

[5] Jun L, Sun G C and Wang J B 2009 *Chin. Phys.* B **18** 1598

[6] Wu T K 1994 *IEEE Trans. Antennas Propag.***42** 1659

[7] Wu T K and Lee S W 1994 *IEEE Trans. Antennas Propag.* **42** 1484

[8] Huang J, Wu T K and Lee S W 1994 *IEEE Trans. Antennas Propag.* **42** 166

[9] Wu T K 1994 *IEEE Trans. Antennas Propag.* **42** 1659

[10] Lockyer D S, Vardaxoglou J C and Simpkin R A 2000 *IEE Proc.-Microw. Antennas Propag.* **147** 501

[11] Romeu J and Rahamat-Samii Y 2000 *IEEE Trans. Antennas Propag.* **48** 1097

[12] Gianvittorio J P, Romeu J, Blanch S and Rahmat-Samii Y 2003 *IEEE Trans. Antennas Propag.* **51** 3088

[13] Gao J S, Wang S S, Feng X G, Xu N X, Zhao J L and Chen H 2010 *Acta Phys. Sin.* **59** 7338 (in Chinese)

[14] Luo G Q, Hong W, Hao Z C, Liu B and Li W D 2005 *IEEE Trans. Antennas Propag.* **53** 4035

[15] Luo G Q, Hong W, Lai Q H, Wu K and Sun L L 2007 *IEEE Trans. Micro. Theory Tech.* **55** 2481

[16] Yang H Y, Gong S X, Zhang P F and Guan Y 2010 *Electron. Lett.* **46** 1

[17] Luo G Q, Hong W, Lai Q H and Sun L L 2008*IET Microw. Antennas Propag.* **2** 23